

<sup>9</sup> Rigdon, W. S., Dirling, R. B., Jr., and Thomas, M., "Radiative and Convective Heating During Atmospheric Entry," DAC-60913, March 1968, Douglas Aircraft Co., MSSD, Santa Monica, Calif.

<sup>10</sup> Olstad, W. B., "Correlations for Stagnation-Point Radiative Heat Transfer," *AIAA Journal*, Vol. 7, No. 1, Jan. 1969, pp. 170-172.

<sup>11</sup> Nicolet, W. E., "Advanced Methods for Calculating Radiation Transport in Ablation-Product Contaminated Boundary Layers," NASA CR-1656, Sept. 1970, Aerotherm Corp., Mountain View, Calif.

<sup>12</sup> Hoshizaki, H. and Lasher, L. E., "Convective and Radiative Heat Transfer to an Ablating Body," *AIAA Journal*, Vol. 6, No. 8, Aug. 1968, pp. 1441-1449.

<sup>13</sup> Kendall, R. M. and Bartlett, E. P., "Nonsimilar Solution of the Multicomponent Laminar Boundary Layer by an Integral-Matrix Method," *AIAA Journal*, Vol. 6, No. 6, June 1968, pp. 1089-1097.

<sup>14</sup> Bartlett, E. P. and Kendall, R. M., "Nonsimilar Solution of the Multicomponent Laminar Boundary Layer by an Integral-Matrix Method," NASA CR-1062, June 1968, Aerotherm Corp., Mountain View, Calif.

<sup>15</sup> Anderson, L. W. and Kendall, R. M., "A Nonsimilar Solution for Multicomponent Reacting Laminar and Turbulent Boundary Layer Flows Including Transverse Curvature," AFWL-TR-69-106, Oct. 1969, Aerotherm Corp., Mountain View, Calif.

<sup>16</sup> Bartlett, E. P. et al., "Further Studies of the Coupled Chemically Reacting Boundary Layer and Charring Ablator,"

NASA CR-92471, Oct. 1968, Aerotherm Corp., Mountain View, Calif.

<sup>17</sup> Deblaye, C. and Bartlett, E. P., "An Evaluation of Thermodynamic and Transport Properties for Use in the BLIMP Non-similar Multicomponent Boundary-Layer Program," Sandia SC-CR-69-3271, July 1969, Aerotherm Corp., Mountain View, Calif.

<sup>18</sup> Hirschfelder, J. O., Curtiss, C. F., and Bird, R. B., *Molecular Theory of Gases and Liquids*, 2nd Printing, corrected, with notes added, Wiley, New York, 1964.

<sup>19</sup> Bartlett, E. P., Nicolet, W. E., and Howe, J. T., "Heat-Shield Ablation at Superorbital Reentry Velocities," Rept. 69-63, Dec. 1969, Aerotherm Corp., Mountain View, Calif.

<sup>20</sup> Kendall, R. M., "A General Approach to the Thermochemical Solution of Mixed Equilibrium-Nonequilibrium, Homogeneous or Heterogeneous Systems," NASA CR-1064, June 1968, Aerotherm Corp., Mountain View, Calif.

<sup>21</sup> Hayes, W. D. and Probstein, R. F., *Hypersonic Flow Theory, Inviscid Flows*, 2nd ed., Vol. 1, Academic Press, New York, 1966.

<sup>22</sup> Woodward, H. T., "Predictions of Shock-Layer Radiation from Molecular Band Systems in Proposed Planetary Atmospheres," TN D-3850, 1967, NASA.

<sup>23</sup> Biberman, L. M., Mnatsakanyan, A. Kh., "Optical Properties of Air in the Temperature Range from 4,000 to 10,000°K," *Teplofizika Vysokikh Temperatur*, Vol. 4, No. 2, March-April 1966, pp. 148-159.

<sup>24</sup> Boison, J. C. and Curtiss, H. A., "An Experimental Investigation of Blunt Body Stagnation Point Velocity Gradient," *ARS Journal*, Vol. 29, No. 2, Feb. 1959, pp. 130-135.

MAY 1971

J. SPACECRAFT

VOL. 8, NO. 5

## An Evaluation of Ablation Mechanisms for the Apollo Heat Shield Material

EUGENE P. BARTLETT\* AND LARRY W. ANDERSON†  
*Aerotherm Corporation, Mountain View, Calif.*

AND

DONALD M. CURRY‡  
*NASA Manned Spacecraft Center, Houston, Texas*

Theoretical ablation solutions for the Apollo heat shield material are compared with data obtained in an arc-plasma tunnel. Some of the more important parameters considered are pyrolysis gas reactivity with the boundary-layer gases, changes in surface elemental composition due to in-depth coking reactions, mechanical removal of candidate surface species, loss of pyrolysis gas through fissures which are seen experimentally to develop in the chars, and surface thermochemistry including silica-carbon reactions. Chemical ablation theory is satisfactory at moderately high surface temperatures if it is assumed that the pyrolysis gases are not effective in blocking the convective heat transfer. At lower surface temperatures, it is necessary to employ a rate law for the mechanical removal of silica in the char material.

### Nomenclature

$B_c'$  = char recession rate normalized by  $\rho_c u_c C_M$   
 $B_g'$  = pyrolysis gas rate normalized by  $\rho_g u_g C_M$   
 $P$  = pressure

$\dot{S}$  = linear surface recession rate

$T_F, T_w$  = fail temperature and surface temperature

$X$  = mole fraction

$\rho_c, \rho_g$  = densities of char and pyrolysis gas

$\rho_c u_c C_M$  = mass-transfer coefficient

### Subscript

$c$  = condensed phase (on chemical element or molecule)

Presented as Paper 69-98 at the AIAA 7th Aerospace Sciences Meeting, New York, January 20-22, 1969; submitted February 11, 1969; revision received January 11, 1971. This work was supported by the NASA Manned Spacecraft Center, Structures and Mechanics Division, under Contract NAS9-6719.

\* Manager, Applied Research Department. Member AIAA.

† Staff Engineer, Applied Research Department. Member AIAA.

‡ Aerospace Engineer. Thermal Technology, Structures and Mechanics Division.

## Introduction

**A**BLATION of reinforced plastics often has been analyzed using the semiempirical heat-of-ablation approach. For the Apollo heat shield material in the Apollo application, however, it has proven better to employ an empirical rate law for surface recession rate  $\dot{S}$  vs wall temperature  $T_w$  at low  $T_w$  and a "carbon" ablation diffusion limit at high  $T_w$ .<sup>1,2</sup> To provide a better understanding of this observed behavior, physicochemical models are postulated, and theoretical predictions from them are compared to ground test data in this paper.

The low-density ablation material, AVCOAT 5026-39/HC-GP, is bonded to a primary structure. It is an epoxy-phenolic resin with phenolic microballoons and silica-fiber reinforcement in a fiber-glass reinforced-phenolic honeycomb matrix. Although this composite maintains its cellular appearance after fabrication, the virgin material is treated theoretically as a continuum. At sufficiently high-heating rates, it chars.

The computer program<sup>3</sup> solves for surface elemental mass balances, producing solutions for ablation rate normalized by mass-transfer coefficient in terms of  $P$ ,  $T_w$ , and normalized pyrolysis gas rate  $B_g'$ . A variety of models can be assumed, including consideration of equilibrium or rate-controlled reactions at the surface and mechanical removal of candidate surface species.

The ground test data considered are those obtained by Schaefer et al.<sup>4</sup> in an arc-tunnel facility for enthalpies from 3000 to 30,000 Btu/lb and local stagnation pressures from 0.008 to 1.0 atm. Comparisons of these data with "limiting" theories, whereby the silica in the char is either permitted to be the surface species or required to fail mechanically if it wants to form the surface species, lead to the proposal of an empirically-derived rate law for mechanical removal of silica.

## Analytical Procedure

The computer program<sup>3</sup> solves for equilibrium chemical composition for a variety of open or closed systems of arbitrary chemical composition. Consideration of any molecular, atomic, ionic, or condensed species requires only the inclusion of the basic thermodynamic data for it. The option of primary interest here is the surface state option, which solves the surface mass balances to determine a relationship among  $B_c'$  (normalized char recession rate),  $B_g'$ ,  $P$ , and  $T_w$ , while considering equilibrium between a char and gases adjacent to it or while considering selected rate-controlled surface reactions. Three useful features of this option are: 1) one does not have to choose a priori the surface species (e.g., the program will determine from the surface equilibrium relationships whether the char surface is  $\text{SiO}_2$ ,  $\text{C}$ ,  $\text{SiC}$ ,  $\text{Si}$ , or

$\text{Si}_3\text{N}_4$ ); 2) each condensed species can be assigned a fail temperature  $T_F$  above which it is not allowed to serve as the surface. (Thus, one can represent mechanical removal of a species which may want to precipitate out but which has poor bonding characteristics or of a species which wants to appear above its melt temperature); and 3) one can isolate species or component gas mixtures from the system or consider rate-controlled surface reactions or surface-catalyzed homogeneous reactions. A principal limitation of the analysis is that the surface is required to consist of a single condensed species, e.g.,  $\text{C}$  (with  $\text{SiO}_2$  and/or  $\text{SiC}$  failing);  $\text{C}$  and  $\text{SiO}_2$ , say, cannot serve simultaneously as the surface material.

The surface state option provides  $B_c'$  and other information needed to perform an energy balance on the surface as a function of normalized  $B_g'$ ,  $T_w$ , and  $P$ ; thus, it does not *by itself* constitute an ablation prediction tool. In the first place, it is necessary to specify the mass-transfer coefficient  $\rho_e u_e C_M$ , and this cannot be done precisely without solving the boundary-layer equations. Secondly, the determination of  $T_w$  requires the solution of a surface energy balance. In the present study, we use experimental<sup>4</sup>  $T_w$ 's, and mass-transfer coefficients are estimated by applying a standard blowing correction to the measured hot wall heat transfer coefficients.<sup>4</sup>

## Summary of Ground Test Data Utilized

Approximately 150 tests of the Apollo heat shield material were conducted in an arc tunnel facility under carefully controlled conditions simulating a broad spectrum of lunar return conditions.<sup>4</sup> Observations during the tests and post-test chemical analyses indicated that there are basically four regimes of surface behavior in terms of  $T_w$  and  $P$ :

- 1) At the lowest  $T_w$ 's (to 1600°K) a surface scab of agglomerated silica fibers appears.
- 2) At 1600° ≤  $T_w$  ≤ 2100°K, silica globules partially cover the char surface, the coverage decreasing as  $T_w$  increases.
- 3) At  $T_w$  > 2100°K, there is no evidence of a silica melt. Although no direct measurements of char density  $\rho_c$  were made, post-test chemical analyses showed substantial decreases in the  $\text{SiO}_2/\text{C}$  ratio near the surface, indicating either a carbon deposit or silica depletion near the surface. Also,  $\text{SiC}$  crystals often showed up in the chemical analysis, but never as more than 2% of the surface material.
- 4) At  $P$  > 1 atm, gross mechanical removal was observed. Other significant findings were that  $\dot{S}$  is independent of run time, and substantial erosion occurs in  $\text{N}_2$  ( $\sim \frac{1}{3}$  that which occurs in air), but only slight erosion occurs in He under similar test conditions.

## Correlation of Surface Thermochemistry Solutions with and without Low Silica Fail Temperature

As discussed previously, a number of decisions have to be made regarding mechanical removal and nonequilibrium considerations, especially for a material as complex as the Apollo material. Strikingly different maps of  $B_c'$  vs  $T_w$  (with  $B_g'$  and  $P$  as parameters) are obtained depending upon whether 1) the pyrolysis gases, based on the elemental composition resulting from primary pyrolysis, are allowed to react at the surface with the char and boundary-layer edge gases or 2) the pyrolysis gases are either allowed to equilibrate with the sub-surface char or are not allowed to react with the char and boundary-layer edge gases. The  $B_g'$  is a dominant parameter in the former (category 1), but takes on only a secondary role in the latter (category 2).

### Category 1: Models with Dominant $B_g'$ Effects

The most straightforward model is to consider the category 1 model, with pyrolysis gas, char, and boundary-layer-edge gases equilibrated at the surface, and to consider all possible

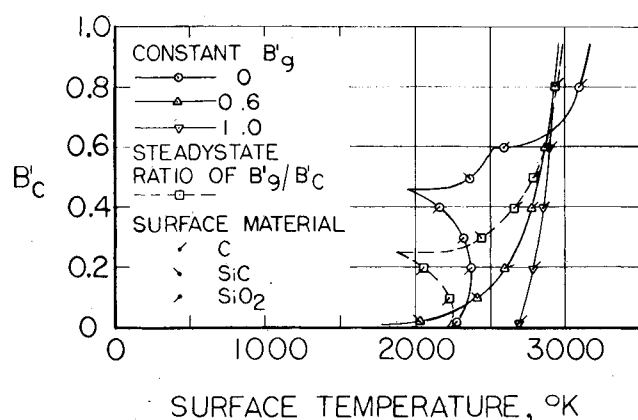


Fig. 1 Surface thermochemistry model for reactive pyrolysis gases ( $P = 0.028$  atm).

candidate surface materials, while imposing no  $T_F$ 's. Based upon chemical analysis and TGA data, the pyrolysis gas and char were assigned densities of 18 and 16 lb/ft<sup>3</sup>, the char being composed of C<sub>c</sub>, SiO<sub>2c</sub>, Al<sub>2</sub>O<sub>3c</sub>, CaO<sub>c</sub>, and B<sub>2</sub>O<sub>3c</sub>. The elemental compositions of the char (char a) and pyrolysis gas are presented in Table 1. The results indicated that the minor constituent aluminum plays an important role in the ablation process. No surface recession was predicted to occur until very high  $T_w$ 's were reached, a surface of Al<sub>2</sub>O<sub>3c</sub> being predicted. These results suggest that there is no chemical means for removing aluminum from the char until the surface becomes hot enough for Al<sub>2</sub>O<sub>3c</sub> to decompose into gaseous products. At higher  $B_c'$ , BN<sub>c</sub>, SiC<sub>c</sub> and finally C<sub>c</sub> were predicted to be the surface species. Another significant feature was that  $B_c'$  was reduced as  $B_g'$  was increased.

It seems unlikely that minor constituents such as Al and B should control  $\dot{S}$ . Rather, one might suspect that they would be carried off in condensed form if there were no means for gasification. Therefore, Al<sub>2</sub>O<sub>3c</sub>, B<sub>2</sub>O<sub>3c</sub>, and CaO<sub>c</sub> were removed from consideration. The approach taken was to replace these species by an equal mass of SiO<sub>2c</sub> to yield the char b and pyrolysis gas compositions of Table 1 while retaining the same  $\rho_c$  and  $\rho_g$ .

The solutions for this model are presented in Fig. 1 for 0.028 atm and several values of  $B_g'$ . Results are also shown for the steady-state  $B_g'/B_c'$  ratio, which is numerically equal to  $\rho_g/\rho_c$ , or 1.125. The constant  $B_g'$  curves are of interest in transient problems. As steady-state ablation is approached, such that the pyrolysis zone moves at the same speed as the receding surface, the steady-state  $B_g'/B_c'$  is attained.

With the minor char constituents removed from consideration, SiO<sub>2c</sub> is predicted to be the surface species under the conditions of low  $B_g'$  and  $B_c'$ . As  $B_c'$  is increased the surface changes to SiC<sub>c</sub> and then C<sub>c</sub>. At higher  $B_g'$ , the SiO<sub>2c</sub> and SiC<sub>c</sub> zones disappear and the surface is C<sub>c</sub> over the entire range of  $B_c'$ . Whether or not SiO<sub>2c</sub> and SiC<sub>c</sub> play such significant roles remains to be seen, but at least silicon is a major component of the char.

The behavior of SiO<sub>2c</sub> parallels the role played by Al<sub>2</sub>O<sub>3c</sub> in the calculations mentioned previously; i.e., there is no chemical means for removing SiO<sub>2c</sub> from the surface until  $T_w$  is sufficiently high that decomposition into SiO and/or Si gas takes place. Surface reaction with C<sub>c</sub> is permitted, resulting, for example, in SiO and CO, but SiO then subsequently reacts with oxygen from the boundary-layer edge to reform SiO<sub>2c</sub>, so there is no net chemical removal of silica from the surface by this process.

There are a number of reasons that one might expect at least some mechanical removal of silica at  $T_w < 2200^\circ\text{K}$  (shown earlier as the  $T_w$  for the onset of thermochemical ablation). First, the silica "melts" at lower temperatures, and there will be some removal by liquid-layer flow. The loss of material by this manner was observed in movies of some of the Schaefer tests (principally for  $1800 < T_w < 2000^\circ\text{K}$ ), and liquid globules were found on the surfaces after cooldown. In addition, experimental data confirm that SiO<sub>2c</sub> and C<sub>c</sub> react at  $T_w$ 's in this same range, and one might

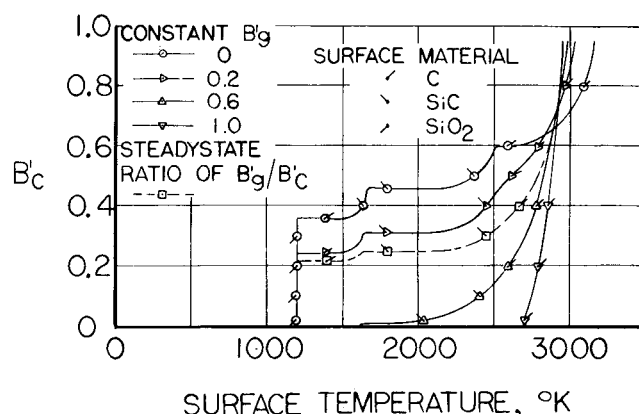


Fig. 2 Surface thermochemistry model for reactive pyrolysis gases with low silica fail temperature ( $P = 0.028$  atm).

expect that the SiO<sub>2c</sub> which reforms at the surface would be mechanically weak.

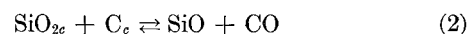
Calculations were performed with an unrealistically low  $T_F$  of  $1200^\circ\text{K}$  for silica, to demonstrate the effect of mechanical removal, if it were to occur, over a wide  $T_w$  range. Solutions for  $P = 0.028$  atm and several values of  $B_g'$  are presented in Fig. 2. The  $B_c'$  curves for the lower  $B_g'$  are extended down to  $T_F$ . The steady-state  $B_c'$  rises to  $\sim 0.22$  at  $T_F$  and then continues to rise slowly with increase in  $T_w$ . The  $B_c'$  is higher for values of  $B_g'$  below the steady-state values and lower for higher  $B_g'$ .

The results of Fig. 2 are readily explainable from the basic physics. Consider first the  $B_g' = 0$  curve where the problem is reduced to one of a homogeneous mixture of SiO<sub>2c</sub> and C<sub>c</sub>. At the lowest  $T_w$ 's all of the silicon in the char is removed mechanically, as the surface recedes, in the form of SiO<sub>2c</sub>. Hence, the problem reduces further to that of carbon ablation. At temperatures slightly above  $T_F$ ,  $B_c'$  has a constant value of 0.362. This is the well-known diffusion limit for



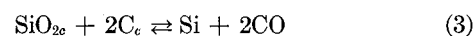
The  $B_c'$  for pure carbon (0.176) is increased to the current value, because the char is only 48.8% by weight carbon. Thus, with a low  $T_F$  for silica, the silica fails at just that rate such that the carbon is exposed and can react with the oxygen which diffuses across the boundary layer. The mechanical removal rate of silica is constant on this plateau.

For  $T_w > 1500^\circ\text{K}$ , SiC<sub>c</sub> becomes the surface species, and vaporization of silica into SiO and O<sub>2</sub> becomes important. Thus, the amount of silica which leaves in the condensed phase begins to decrease, and the oxygen released by the silica vaporization becomes available for reaction with carbon. The net effect is



The carbon consumed in this process is in addition to the carbon consumed by the oxygen from the free stream. Thus,  $B_c'$  increases as  $T_w$  (and, hence, the vaporization rate of SiO<sub>2c</sub>) is increased.

At  $\sim 1700^\circ\text{K}$ , the decomposition rate of SiO<sub>2c</sub> is sufficient to remove the silicon from the char at the same rate that carbon is consumed by reactions (1) and (2). Thus, the mass removal rate of SiO<sub>2c</sub> is reduced to zero and another plateau region is achieved, with  $B_c' = 0.458$ . As  $T_w$  is elevated still further, the SiO<sub>2c</sub> decomposes into Si and O<sub>2</sub> yielding the net reaction



Twice as much carbon is consumed through this decomposition reaction as through reaction (2). Thus, another plateau

Table 1 Char and pyrolysis gas elemental mass fractions, a) considering and b) neglecting minor constituents in char

Element	Pyrolysis gas	Char a	Char b
H	0.0930	...	...
B	...	0.0079	...
C	0.5470	0.4880	0.488
N	0.0190	...	...
O	0.3410	0.2605	0.273
Al	...	0.0212	...
Si	...	0.1852	0.239
Ca	...	0.0366	...

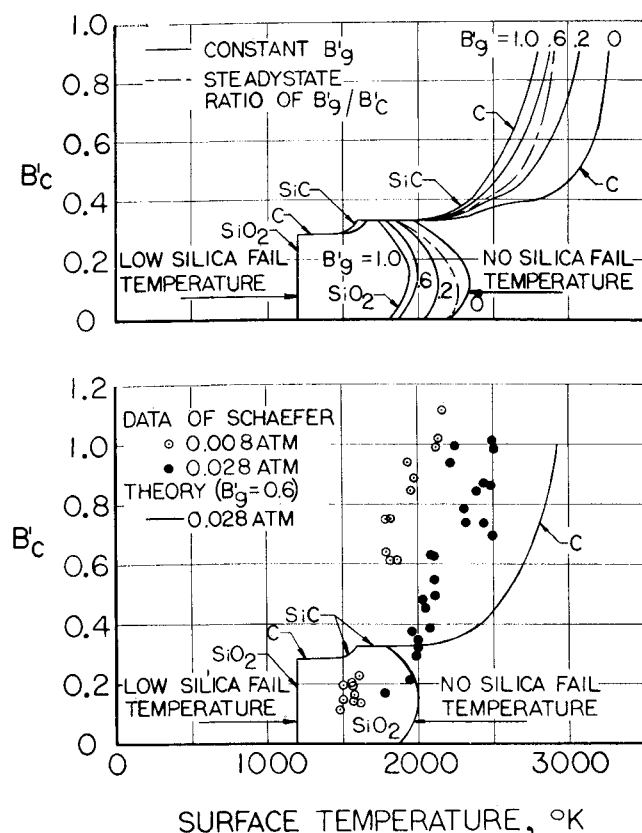
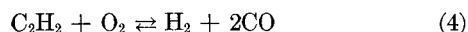


Fig. 3 Surface thermochemistry model for reactive pyrolysis gases considering coking ( $P = 0.028$  atm), and comparison with ground test data.

would be anticipated with  $B_g' = 0.62$  if the concentration of SiO were to become vanishingly small compared to Si.

At  $T_w > 2500^\circ\text{K}$ , sublimation of carbon and reaction with  $\text{N}_2$  to form CN become important, and a distinct plateau is not seen for the pressure considered. At  $T_w > 2800^\circ\text{K}$ ,  $B_g'$  rises sharply as sublimation becomes more important.

The reduction of  $B_g'$  with increase in  $B_g'$  can be attributed to the way the virgin material is distributed into pyrolysis gas and char (char b in Table 1), carbon in the pyrolysis gas exceeds that required for equilibrium. At the surface in the carbon-plateau region, the only abundant species containing carbon is CO, whereas the C/O ratio in the original pyrolysis gas is considerably higher, being in the form of various hydrocarbons. Thus, in order to achieve the surface gas composition, reactions of the form



are proceeding to the right. The net effect is that pyrolysis gas being supplied from the decomposition zone consumes oxygen from the boundary layer edge without contributing to surface recession.

The reactive pyrolysis gas surface recession model considering a low  $T_F$  for silica was applied to a number of the ground tests of Schaefer et al.<sup>4</sup> Maps of  $B_g'$  for various  $B_g'$  and  $T_w$  were generated for the test conditions and were employed as inputs to a two-moving-boundary conduction program<sup>5</sup> to predict transient ablation rates and temperatures. The most striking results are that the total surface recession is substantially underpredicted, and the predicted  $\dot{S}$  is strongly dependent on time. (In contrast, as discussed previously, the measured  $\dot{S}$  is insensitive to time.) This predicted behavior can be attributed directly to the high  $B_g'$  values, which decrease asymptotically from  $\sim 2.0$  early in the test to  $\sim 0.5$  at the end.

A transient ablation prediction was also made for a recent Apollo superorbital flight using this model (with low  $T_F$  for silica). Consistent with the ground-test correlations, the prediction for total recession was an order of magnitude low. Clearly, this reactive pyrolysis gas surface thermochemistry model is inadequate. In particular, the problem appears to lie in the dominant effect of  $B_g'$  on the surface recession.

## Category 2: Models without Dominant $B_g'$ Effects

One could postulate several models which would tend to eliminate the strong  $B_g'$  effect. First, recalling that it is the carbon in the pyrolysis gas in excess of that required to convert the oxygen in the pyrolysis gas to CO that produces the strong  $B_g'$  effect, one might consider a different elemental composition of char and pyrolysis gas, transferring carbon from the pyrolysis gas to the char. Secondly, reactions between the pyrolysis gas, char, and boundary layer gases may not proceed to equilibrium. Thirdly, the pyrolysis gas may not mix thoroughly with the other gaseous species.

Experimental evidence qualitatively supports the first and third of these possibilities. Flight data for the Apollo material<sup>6,7</sup> have shown that there is a substantial increase in carbon density near the surface, obviously due to in-depth coking reactions. Secondly, both ground<sup>4</sup> and flight test data<sup>7</sup> for this material have shown numerous fissures in the char. One could speculate that a bulk of the pyrolysis gas might pass out through these fissures and jet, for the most part, out through the boundary layer without mixing with the boundary-layer gases. These three models will be considered in the order listed. Surface thermochemistry maps will be generated and compared to the ground test data of Schaefer et al.<sup>4</sup>

## Reactive pyrolysis gases considering coking

The effect of coking was treated approximately by removing all of the carbon from the pyrolysis gas in excess of that needed to convert the oxygen in the pyrolysis gas to CO and assigning this excess carbon to the char elemental composition and density. The resulting elemental compositions are shown in Table 2;  $\rho_c$  is increased from 16.00 to 21.24 lb/ft<sup>3</sup>, while  $\rho_g$  is correspondingly decreased. Solutions for  $P = 0.028$  atm and a range of  $B_g'$  are presented in Fig. 3a and can be compared to the noncoking results of Fig. 2. The results for steady-state ratios of  $B_g'/B_c'$  are also indicated on these figures.

As expected, the coking model yields plateau behavior with little effect of  $B_g'$  for  $T_w < 2200^\circ\text{K}$ ; all of the carbon in the pyrolysis gas is tied up in CO, so that the gas is neutral. In the steady-state limit, the coking and noncoking models yield identical results for surface recession of the virgin material,  $B_g' + B_c'$ . This, of course, must be the case, since the composition of the virgin material is the same for both models.

To facilitate comparison of theoretical models to the data of Schaefer, the following approach is used. First, solutions are shown only for  $B_g' = 0.6$ , because for a number of transient predictions for the test conditions of Schaefer for various models, the  $B_g'$  values consistently rise to a maximum of about 2 to 4 but then drop rather quickly in the test to a value

Table 2 Char and pyrolysis gas elemental mass fractions considering equilibrium coking

Element	Pyrolysis gas	Char
H	0.1311	...
C	0.3614	0.614
N	0.0268	...
O	0.4807	0.206
Si	...	0.180

of 0.8 to 0.4. Secondly, data are presented for both 0.008 and 0.028 atm, whereas theory is shown only for 0.028 atm. The theoretical effect of a decrease in pressure from 0.028 to 0.008 atm is typically to move sublimation and vaporization curves to  $T_w$ 's which are 100 to 200°K lower, whereas values of  $B_c'$  on the various plateaus are independent of pressure.

The data of Schaefer, reduced to  $B_c'$  vs  $T_w$ , are compared to the coking theoretical model in Fig. 3b. One can conclude that either most of the experiments were conducted in the sublimation regime and experimental and analytical uncertainties combine to yield a 500 to 800°K discrepancy, or that the data lie well above the "upper limit" prediction. There is good reason to believe that the former is not the case, in which case one must conclude that this model is unsatisfactory. In the first place, liquid globules were detected in many of these tests, attesting to the validity of the measured surface temperatures, and hardly being indicative of sublimation temperatures. Secondly, the transient solutions indicated that there is not sufficient energy available to achieve sublimation conditions.

### Frozen pyrolysis gases

At relatively low  $T_w$ 's one might expect that the pyrolysis gases would not equilibrate with the char and boundary-layer gases at or near the surface. The feedback to the surface of the effect of reactions farther into the boundary layer is relatively small. Therefore,  $B_c'$  maps were generated for a frozen pyrolysis gas having the following conjectured molar composition:  $X_{C_2H_4} = 0.30$ ,  $X_{CO} = 0.20$ ,  $X_{CH_4} = 0.15$ ,  $X_{C_2H_2} = 0.15$ ,  $X_{H_2O} = 0.15$ ,  $X_{N_2} = 0.04$ , and  $X_{H_2} = 0.01$ . This composition is consistent with the elemental composition of the pyrolysis gas (Table 1) and is believed to represent reasonable estimates of species which might be expected for this material.

The predictions (Fig. 4a) for  $P = 0.028$  atm, and  $B_g' = 0$  and 1, show that  $B_g'$  has no effect in the various plateau regions and only a minor effect in nonplateau regions. Furthermore, the plateau values of  $B_c'$  are higher than in the case considered previously (where the pyrolysis gas was inert because of in-depth coking), because carbon in the pyrolysis gas is removed from the virgin material in the present model without requiring it to react.

The predictions are compared to the data in Fig. 4b, together with another prediction to be discussed later. The experimental  $B_c'$  points are lower than in the coking model because, for a given  $\dot{S}$ , the  $\dot{m}_c$  is lower due to a lower  $\rho_c$ . Also, as discussed previously, the prediction for  $B_c'$  is higher. However, many of the data points are still underpredicted.

For  $1400^\circ \leq T_w \leq 2580^\circ K$ , the predicted surface species is  $SiC_x$ . However, post-test chemical analyses of char material have indicated very little  $SiC_x$ . Therefore, surface thermochemistry calculations also were performed with  $SiC_x$  removed from consideration, implying that the formation of  $SiC_x$  is kinetically-limited. The effect on the solution was small (as long as  $Si_3N_4$  is also removed from consideration), the  $B_c'$  being increased for  $T_w$  of  $1800^\circ$  to  $2580^\circ K$  but by no more than 5%.

Maps also were generated considering a low  $T_F$  (1200°K) for  $SiC_x$ . Solutions for  $B_g'$  of 0.6 and  $P = 0.028$  atm are also presented in Fig. 4b. The low  $T_F$  for  $SiC_x$  has a dramatic effect on the predictions for  $1400^\circ \leq T_w \leq 2580^\circ K$ ; namely, the  $B_c'$  is approximately doubled over most of the region where  $SiC_x$  wants to be the surface species.

To provide further insight into these results, the following discussion is offered. Starting at the 1200°K fail temperature for  $SiO_{2c}$ , the surface is  $SiO_{2c}$ , which is failing. As  $B_c'$  is increased, the  $SiO_{2c}$  removal rate increases until it attains a maximum at the carbon plateau value of  $B_c' = 0.362$ . The surface then changes to carbon, and  $B_c'$  remains constant to  $T_w \approx 1400^\circ K$ , at which point equilibrium dictates that silica-

carbon reactions become significant:



As this reaction begins to move to the right,  $SiC_c$  forms and fails and less  $SiO_{2c}$  is available to fail. At the peak  $B_c'$  of 0.972, the surface is still  $C_c$ , and mechanical removal is all in the form of  $SiC_c$ , meaning that reaction (5) has gone to completion. Here the carbon is oxidized by the boundary-layer edge gas and all of the oxygen in the silica, and carbon also is being removed mechanically via  $SiC_c$ . As  $T_w$  is increased, the  $SiC_c$  removal rate (and hence the  $B_c'$ ) drop until  $T_w = 2580^\circ K$ ,  $B_c' = 0.609$ , and mechanical removal is zero. This decrease in  $B_c'$  is the result of  $SiC_c$  decomposition into gaseous products, less carbon being carried away in the form of  $SiC_c$ .

The theoretical model for frozen pyrolysis gases with low  $SiC_c$  fail temperature encompasses all of the Schaefer data points for the two pressures considered in Fig. 4b, as discussed later.

### Fissure model

Photomicrographs (15X) of char samples from a recovered Apollo flight vehicle<sup>7</sup> and from Ref. 4 revealed sizeable fissures in many of the char segments between the honeycomb walls. These fissures appear to lead from the decomposition zone to the surface. Thus, the pyrolysis gases, instead of passing homogeneously through the char, may flow, for the most part, along the fissures and pass inefficiently through the boundary layer. With regard to thermochemical ablation theory, the results presented previously for  $B_g' = 0$  are directly applicable. However, there is a major difference when it comes to applying these results to determine  $\dot{m}_c$ ; namely, in the fissure model there is assumed to be no reduction of the convective heating rate by the pyrolysis gas. Thus,  $\rho_c u_c C_M$  and  $\dot{m}_c$  are higher for the same  $B_c'$ .

The data<sup>4</sup> are compared to the fissure model in Fig. 5. The disallowance of a blowing correction for  $B_g'$  substantially

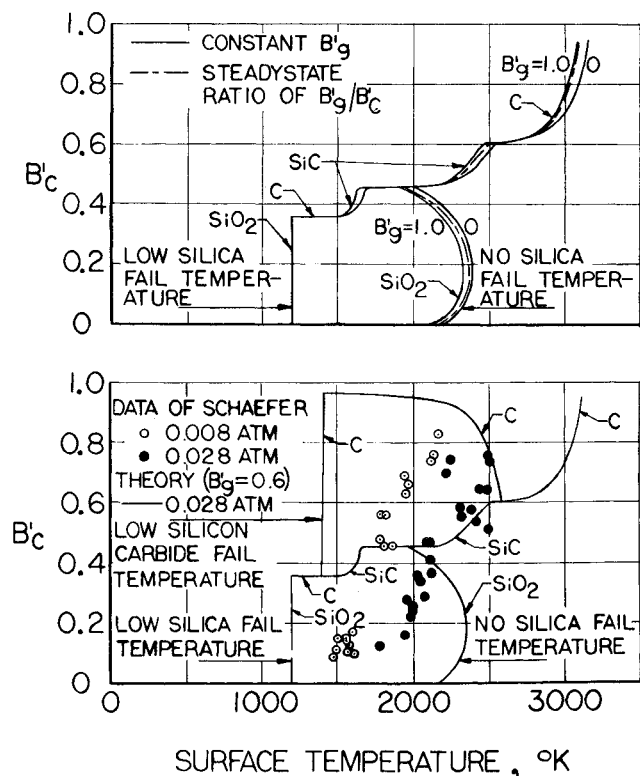


Fig. 4 Surface thermochemistry model for frozen pyrolysis gases ( $P = 0.028$  atm), and comparison with ground test data.

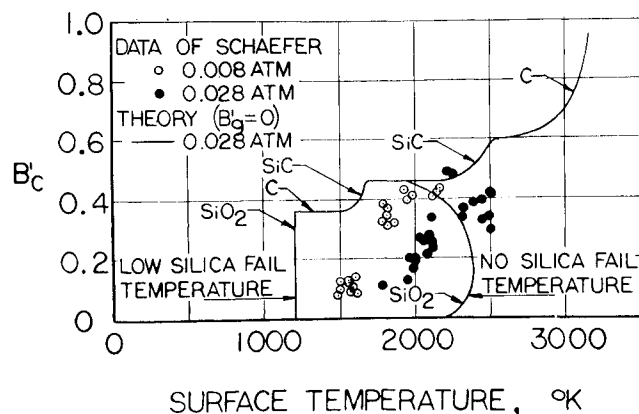


Fig. 5 Correlation of fissure surface thermochemistry model with ground test data.

increases the experimental  $\rho_e u_e C_M$  and thus decreases the experimental  $B_c'$  (for the observed  $\dot{S}$ ) relative to nonfissure models. As a result, all data are encompassed by the upper and lower-limit theories relative to the status of the silica in the char.

#### Discussion of Results

Two major conclusions from the foregoing results are: 1) there must be a mechanism for mechanical removal of silica, since a number of the tests show substantial ablation at  $T_w$ 's well below those corresponding to silica decomposition (a rate law for the mechanical removal of silica is presented later); and 2) there must be a means by which carbon is removed in excess of that which can be consumed by reaction with oxygen in the boundary layer and in the silica. Two possible mechanisms are the formation and mechanical removal of  $\text{SiC}_e$  and the loss of pyrolysis gases (which contain carbon which would otherwise have to react) because of fissures which form in the char.<sup>§</sup> The data examined to this point do not permit a definitive choice between these models. Both envelop the Schaefer data between solutions with and without silica failing. Fissures have been observed in post-test chars, but so have traces of  $\text{SiC}_e$ . Intuitively, the fissure model is somewhat more satisfying and thus is tentatively selected as being more likely; a limited number of correlations with flight test data give encouraging results.<sup>8</sup>

#### Development of Rate Law for Removal of Silica at Low Surface Temperatures

It remains to attempt to rationalize the experimental data which lie, for the most part, between the solutions for silica failing and not failing. Recalling that the use of a fail temperature provides a means for mechanical removal of a condensed species which wants to serve as the ablating surface, it is clear that some silica is removed mechanically, but not so much as to permit diffusion-controlled ablation of carbon. The mechanical removal of silica from the Apollo heat shield material is believed to be a complex interrelationship between kinetically-controlled silica-carbon reactions, melting with subsequent liquid layer removal, and possibly mechanical erosion.

There is an equilibrium potential for silica-carbon reactions at relatively low temperatures, but kinetics limit the rate at which this reaction proceeds for  $T_w < 2000^\circ\text{K}$  or so.

§ As an alternative means for reducing the effects of blowing on the convective heating, an empirical coking model has been used with good success by Curry et al.<sup>1</sup> in analyzing Apollo flight test results. Alternative means for carbon removal by mechanical erosion or nitrogen attack have been shown<sup>8</sup> to be unlikely.

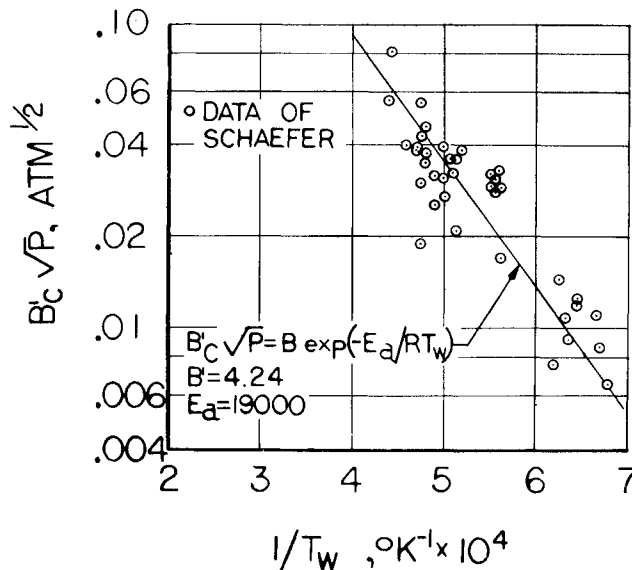
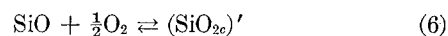


Fig. 6 Correlation of Schaefer ground test data in terms of  $B_c' P^{1/2}$ .

Thus a reaction such as Eq. (2) is taking place in the char layer at and near the surface. However, in the  $T_w$  range for which a  $\text{SiO}_{2c}$  recession model is desired, the  $\text{SiO}$  will react with oxygen from the boundary layer to reform condensed-phase silica, designated  $(\text{SiO}_{2c})'$  to distinguish it from the original silica in the material:

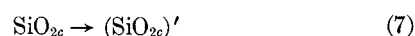


Thus, in the actual case one would expect reaction (2) to proceed at some finite rate and to act together with reaction (6) to produce a net attack of carbon by the oxygen in the boundary layer. This would be expected to produce a gradual buildup of a  $(\text{SiO}_{2c})'$  layer over a receding subsurface consisting of the original  $\text{SiO}_{2c}$  and  $\text{C}_e$  if the  $(\text{SiO}_{2c})'$  that forms (or original  $\text{SiO}_{2c}$  for that matter) does not flow or slough off.

One may well ask, then, why zero surface recession is predicted with the present analytical procedure unless silica is removed mechanically. The answer lies in the fact that the analysis<sup>3</sup> considers only the surface and, at this surface, allows only one condensed phase to exist. In the calculations reported in previous sections, there is no distinction made between  $\text{SiO}_{2c}$  and  $(\text{SiO}_{2c})'$ . Therefore, if  $\text{SiO}_{2c}$  is not allowed to fail, it is predicted to be the surface, and zero surface recession is predicted.

Since the prediction of zero surface recession in the absence of a low  $T_F$  for silica is the result of a limitation in the present analysis, it is well to perform independent calculations to ascertain whether or not surface recession can be explained on the basis of silica-carbon kinetics alone, with the net effect being the recession of an inner surface under a redeposited silica layer. This is done in Ref. 8 for the  $T_w$  range ( $1400^\circ$ – $1640^\circ\text{K}$ ) where a siliceous scab covers the surface. Applying generally-accepted kinetic coefficients for silica-carbon reactions, it is shown therein that reaction rates are insufficient to explain  $\dot{S}$ 's in this  $T_w$  range on the basis of silica-carbon kinetics alone.

To simulate the redeposited silica layer with the present analytical procedure,<sup>3</sup> it is necessary to distinguish between the silica in the original material and the redeposited silica. The silica in the surface material is allowed to communicate with the boundary-layer gases only through the one-way reaction



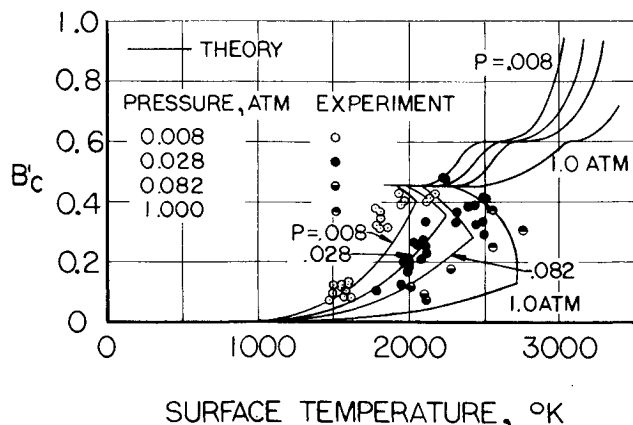


Fig. 7 Comparison with ground test data of fissure surface thermochemistry model including  $B_c'P^{1/2}$  correlation for mechanical removal of silica.

The  $(\text{SiO}_{2c})'$  is considered to be in equilibrium with the boundary-layer gases and is assigned a low  $T_F$ . In effect, then, the silica in the surface material is considered to be converted to  $(\text{SiO}_{2c})'$  at just that rate such that the  $(\text{SiO}_{2c})'$  which forms will fail so as to yield the experimentally observed  $B_c'$ .<sup>8</sup>

To develop an analytical expression for a rate law for reaction (7) the data of Fig. 5 which lie to the left of the silica vaporization curves are plotted in Fig. 6 as  $\log (B_c'P^{1/2})$  vs  $1/T_w$ . A straight line fits the data quite well. It can be represented by

$$B_c'P^{1/2} = B \exp (-E_a/RT_w) \quad (8)$$

where  $B = 4.24$  and  $E_a = 19,000$  with  $T_w$  in °K and  $P$  in atm. The resulting surface thermochemistry solutions in Fig. 7 show that the empirical fit of the low- $T_w$  data and thermochemical ablation theory correlate the ground-test data quite well.

With respect to extension of this correlation to flight conditions, the primary question is whether the rate law for mechanical removal of silica should be applied to flight as  $B_c'$  vs  $T_w$ , or as  $\dot{S}$  vs  $T_w$ .<sup>†</sup> There is considerable distinction between these two approaches because of the order-of-magnitude difference in size between ground-test models and the full-scale Apollo vehicle. In particular, application of an  $\dot{S}$  vs  $T_w$  correlation of the Schaefer data to the full-size Apollo vehicle shifts the ablation threshold to  $T_w$ 's  $\sim 500^\circ\text{K}$  lower.<sup>8</sup>

If the empirical rate law were strictly a rate law representing the kinetics of the silica-carbon reaction, one might favor the  $\dot{S}$  correlation. However, it should be recalled that it is

more probably a rate law for representing the mechanical removal of silica. If melting is the controlling process, the  $B_c'$  correlation might be more meaningful, because the viscosity of silica is strongly temperature-dependent. It is believed that the real situation is intermediate but nearer the  $B_c'$  correlation.

The fissure model has been applied to recent superorbital flight data using both approaches.<sup>8</sup> The  $B_c'$  correlation resulted in substantial agreement for total recession and  $T_w$ 's for the single body point and flight considered, whereas the  $\dot{S}$  correlation substantially overpredicted total recession.

## Concluding Remarks

A systematic study of ground test data for the Apollo heat shield material has suggested that: 1) at relatively low surface temperature  $T_w$ , mechanical removal of silica occurs which can be correlated by an Arrhenius-type relation, and 2) the pyrolysis gases are not effective in reducing convective heating (presumably as a result of fissures in the char). Although this model correlates quite well the ground and flight test data which have been examined, it should not be inferred that it is necessarily the correct ablation model. It is not entirely clear whether the silica rate law should be interpreted as  $\dot{S}$  vs  $T_w$  or as  $B_c'P^{1/2}$  vs  $T_w$ , and the behavior at high  $T_w$ 's could be interpreted as mechanical removal of  $\text{SiC}_c$  and/or  $\text{C}_c$  rather than the result of nonuniform pyrolysis gas flow due to fissures.

## References

- Curry, D. M. and Stephens, E. W., "Apollo Ablator Thermal Performance at Superorbital Entry Velocities," TN D-5969, 1970, NASA.
- Walton, T. E., Jr., Witte, W. G., and O'Hare, B. J., "Flight Investigation of the Effects of Apollo Heat-Shield Singularities on Ablator Performance," TN D-4791, Sept. 1968, NASA.
- Kendall, R. M., "A General Approach to the Thermochemical Solution of Mixed Equilibrium-Nonequilibrium, Homogeneous or Heterogeneous Systems," CR-1064, June 1968, Aerotherm Corp., Mountain View, Calif., NASA.
- Schaefer, J. W. et al., "Experimental and Analytical Evaluation of the Apollo Thermal Protection System Under Simulated Re-entry Conditions," Rept. 67-16, Parts I and II, July 1967, Aerotherm Corp., Mountain View, Calif.
- Moyer, C. B. and Rindal, R. A., "Finite Difference Solution for the In-Depth Response of Charring Materials Considering Surface Chemical and Energy Balances," CR-1061, June 1968, Aerotherm Corp., Mountain View, Calif., NASA.
- Ihnat, M. E., "Evaluation of the Thermophysical Properties of the Apollo Heat Shield," AVSSD-0375-67-RR, Aug. 1967, Avco Space Systems Div., Wilmington, Mass.
- Alexander, J. G. et al., "Evaluation of the Thermophysical Properties of the Apollo Heat Shield, AS-501 Flight Core Study," AVSSD-0206-68-RR, July 1968, Avco Space Systems Div., Wilmington, Mass.
- Bartlett, E. P. and Anderson, L. W., "An Evaluation of Ablation Mechanisms for The Apollo Heat Shield Material," NASA CR-92472, Oct. 1968, Aerotherm Corp., Mountain View, Calif.

<sup>†</sup> Predictions<sup>1</sup> based on a  $\dot{S}$  -  $T_w$  correlation (also diffusion-limited) and an empirical rate law for coking, without considering fissures, have agreed well with flight data.